Analytical and finite element design optimisation of a tubular linear IPM motor

N. Bianchi
Department of Electrical Engineering, University of Padova, Padova, Italy
A. Canova, G. Gruosso and M. Repetto
Department of Electrical and Industrial Engineering, Politechnic of Torino, Torino, Italy, and
F. Tonel
Department of Electrical Engineering, University of Padova, Padova, Italy

Keywords *Optimisation, Finite element, Linear motors, Design*

Abstract *The optimisation of a tubular linear motor with interior permanent magnets is described. For a rapid design the whole process is divided in three parts: an analytical approach for the a preliminary investigation, a parametric analysis by means of a finite element method and an optimisation. The obtained results show that the adopted optimisation process is efficient for rapid and effective optimisation of the tubular linear motor.*

I. Introduction

This paper deals with the optimisation design of a tubular linear motor, with interior permanent magnets (TLPM). This kind of motor is used for linear motions, exhibiting high force-to-volume ratios and high positioning speed. Supply current is injected in stator coils that can be either housed in slots or can be placed directly on stator yoke. Thus two structures can be analysed and will be referred as slotted and slotless TLPM.

The approach to the optimised design of a TLPM motor is split into the following three parts:

(1) The first part is based on the prediction of the motor performance by an analytical approach. It takes into account some constraints in the tubular linear motor design such as given external dimensions, thermal, magnetic limits, etc., and highlights the main design parameters which influence its performance: permanent magnet-to-airgap thickness ratio, inner-to-external diameter ratio and so on. This design process is applied to both slotted and slotless stator structure.

(2) The second part deals with the comparison by means of finite element (FE) analysis of two TLPM motors, slotted and slotless motors, designed in the first part. The aim is the validation of analytical design and the extension to the non-linear behaviour of materials.

(3) Finally, an optimisation of TLPM is carried out, by means of the FE method coupled to one deterministic optimisation procedure. In this

COMPEL : The International Journal for Computation and Mathematics in Electrical and Electronic Engineering, Vol. 20 No. 3, 2001, pp. 777-795

optimisation process, a multiobjective problem is considered, taking into account different motor performances as mean axial force and ripple force.

II. TLPM motor structure

Two different construction types can be selected for TLPM motors, that is the slotted and the slotless structure. In Figures 1 and 2 a sketch of the cross section in these two types is shown together with their main geometrical dimensions.

III. Analytical design

The first step of the proposed procedure is performed to find out which are the geometrical parameters most influencing the performances of the device. Engineering constraints are taken into account and in particular:

- thermal constraints are considered by means of maximum value of current density in the winding. In fact, the area of the external surface of the motor limits the amount of Joule losses that the motor is able to dissipate;
- magnetic constraints such as permanent magnet demagnetisation and saturation of stator magnetic circuit are taken into account fixing a desired value of magnetic flux density.

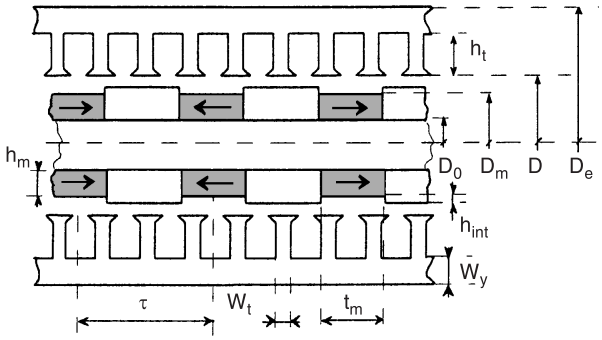

Figure 1.
TLPM slotted structure

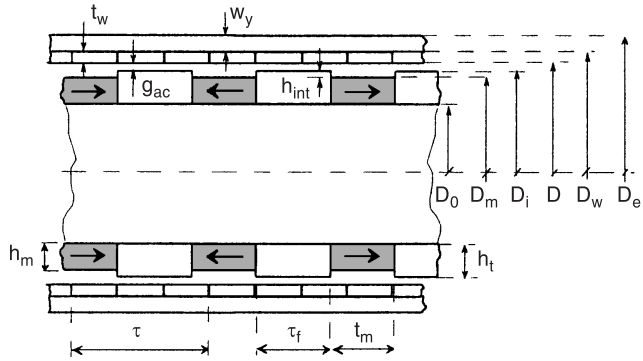

Figure 2.
TLPM slotless structure

Using the analytical equations, obtained for linear magnetic materials, and the constraints mentioned above, some sensitivity analysis can be performed finding out the best set of the motor geometrical parameters.

For instance, Figure 3 shows the force-to-volume ratio versus the inner-to-external diameter ratio, say D/D_e, of two linear motors with interior NdFeB permanent magnets, while Figure 4 shows the force-to-volume ratio, F/Vol, of a D_e = 80mm slotted motor varying the magnet radial height h_m. A detailed description of the analytical procedure is reported in Bianchi *et al.* (2000).

III. FEM model

Once a set of parameters has been defined by step 1 of the proposed method, a validation of the results obtained versus a 2D FEM code is performed, assessing the degree of reliability of the analytically predicted performances. This time, the structure of the motor is described in full detail taking into

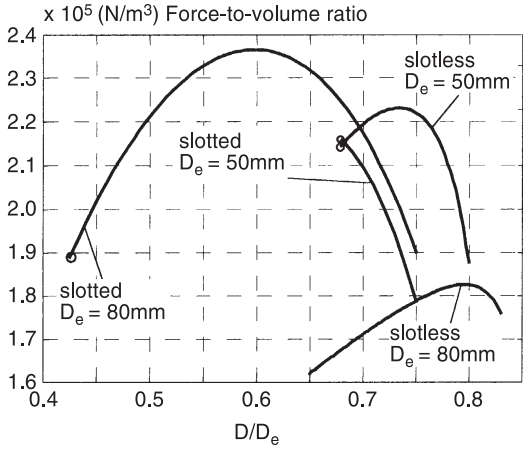

Figure 3.
Force-to-volume ratio versus the inner D-to-external D_e diameter ratio

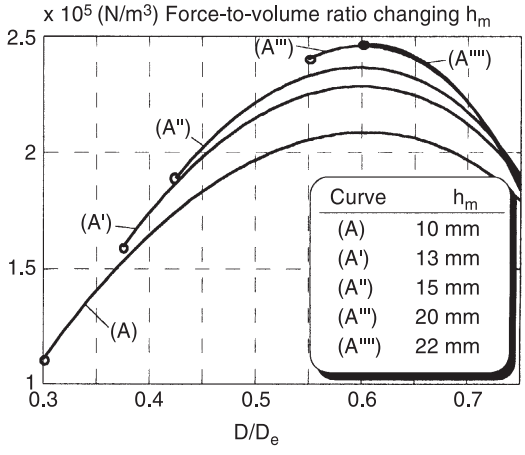

Figure 4.
Force to volume ratio of a slotted motor varying the magnet radial height h_m

account also nonlinearity due to ferromagnetic materials. The same parameters defined in step 1 could be used, thus making comparisons between analytical and numerical predictions straightforward.

The field problem is solved by a magnetostatic formulation in an axi-symmetric domain which can be reduced through periodic conditions. A set of field problems for different cursor positions (synchronous to the stator field) is solved. The cursor displacement must be checked in order to verify the quality of the mesh inside the airgap. To solve this problem a proper routine generates for each position a new airgap mesh. Moreover, for each cursor position, direct and quadrature axis currents are calculated from a fixed current and a load angle. The current intensity is imposed by the thermal constraint while supply conditions (load angle) are set to the theoretical maximum force.

1. Slotted TLPM motor

In the validation part the comparison is focused on local and integral quantities. A first analysis regards the magnetic flux density inside the domain. For instance, Figure 5 shows a comparison between the radial magnetic flux density distribution versus the z-axis coordinate of the cursor, calculated by FEM and by analytical method, highlighting the good agreement between the two analyses. In Figure 6 an example of magnetic field plot at no-load conditions is reported.

Moreover, the FEM model allows the evaluation of the axial component of the flux density which can slightly modify the magnetic behaviour (Figure 7). The main design parameter values adopted for the comparison are reported in Table I, column (a).

Finally the comparison of the axial force completes the validation of the analytical method. In Figure 8 the FEM axial force versus cursor position is compared to the analytical one. The figure shows again a close agreement between the results of the two analyses. However, only the FEM is able to

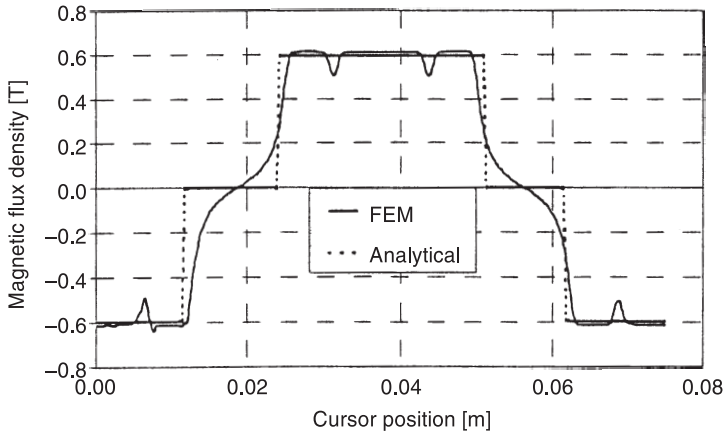

Figure 5.
Radial magnetic flux density in the airgap under no-load operation

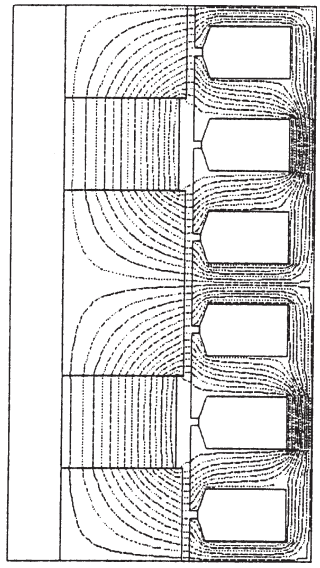

Figure 6.
Magnetic flux plot under no-load operation

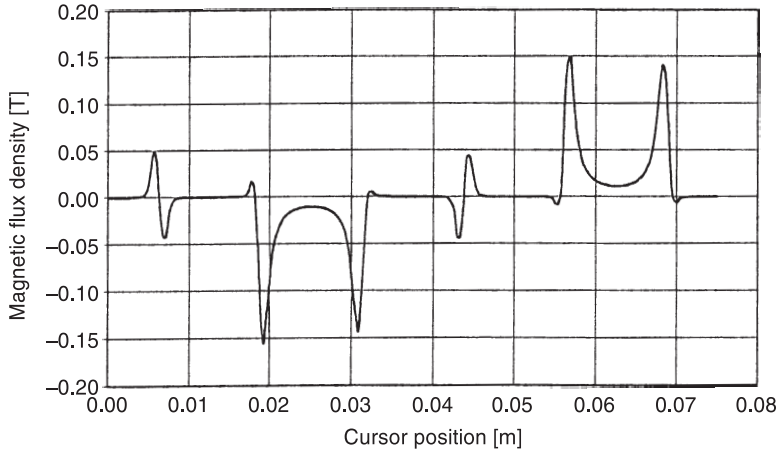

Figure 7.
Axial magnetic flux density in the airgap under no-load operation

determine anisotropy effects due to stator slotting and the related ripple force, as well as the space harmonics effects due to the concentrated coils.

2. Slotless TLPM motor

The same comparison performed for the slotted machine has been carried out for the slotless structure. The main design data of the motor used in the comparison are reported in Table I, column (b). Figure 9 shows a magnetic flux plot distribution under no-load operation. The comparison between FEM and analytical method is shown in Figures 10 and 11. Either radial magnetic flux density or axial force, which practically does not present ripple torque, shows a good agreement between the two procedures.

Parameter	Value (a) slotted (mm)	(b) slotless (mm)
D_e	80	50
D	48	36
W_t	5.48	–
W_s	7.02	–
W_y	3.36	2.24
G_{ac}	1	1
H_{int}	1	1
H_m	15	12
τ	37.5	37.5
T_m	12.5	20.5
D_i	46	34
D_m	44	32
D_0	14	8
τ_f	25	17
h_t	12.64	–
t_w	–	4.76
Q	24	24
2p	8	8

Table I.
Slotted and slotless tubular linear IPM motor design parameters

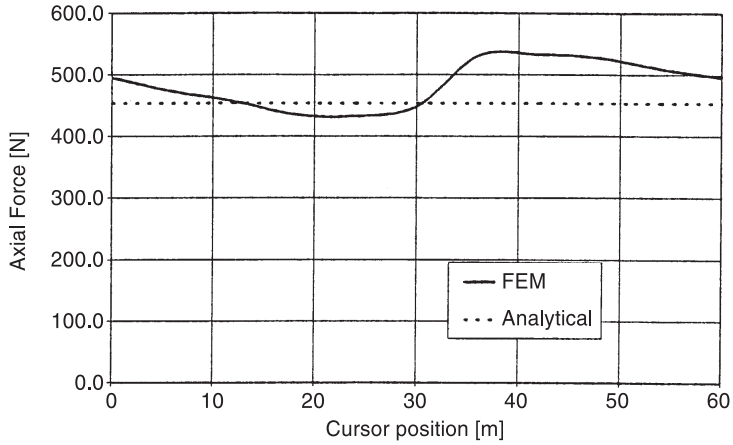

Figure 8.
FEM and analytical axial force versus cursor position (I_d = 0 *A*; I_q = 382 *A*)

IV. FEM optimisation design of slotted TLPM motor

The third and last step of the procedure takes into account a thorough optimisation of the TLPM.

Several design parameters play an important role in the definition of device performances. In particular our study has been focused on those parameters which influence the force behaviour (average and ripple amplitude). In order to reduce the high number of parameters, suitable ratios between motor dimensions, reported in Figure 12, have been introduced together with external volume constraint. All the motor dimensions are the calculated from the introduced optimisation parameters through the formula reported in Appendix A.

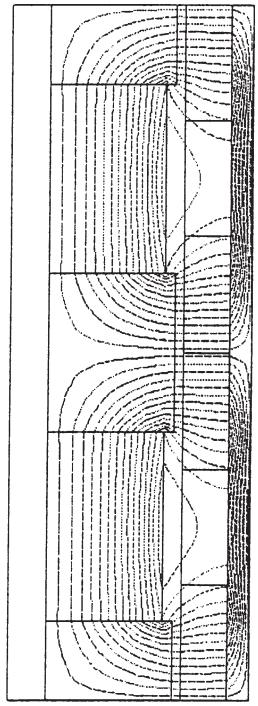

Figure 9.
Magnetic flux plot under no-load operation

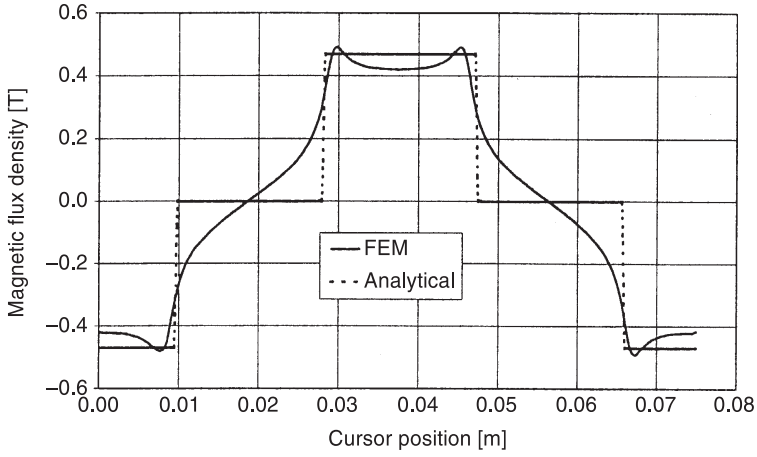

Figure 10.
Radial magnetic flux density in the airgap under no-load operation

The optimisation process is multi-objective and is dealt with by means of a deterministic zero-th order method with scalarisation of objective function by means of fuzzy logic membership functions (Chiampi *et al.*, 1996; Canova *et al.*, 1998). The choice of a deterministic method is due to the calculation time of the optimisation objective. In fact, the evaluation of the axial force behaviour versus cursor position requires at least eight or ten non-linear field solutions (one for

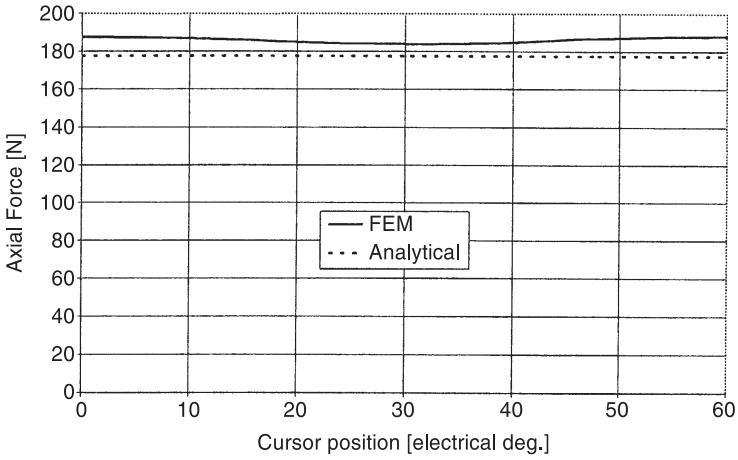

Figure 11.
FEM and analytical axial force versus cursor position (I_d = 0 A; I_q = 336 A)

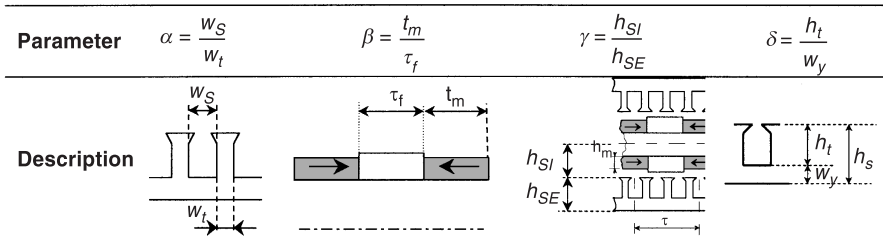

Figure 12.
Optimisation parameter

each cursor position in the periodic interval of a stator slot pitch) and each of them takes about one minute of CPU on a Compaq Alpha Station 667 MHz.

1. Parameter analysis

Before starting with the FEM optimisation it is important to carry out a parametric analysis which outlines the influence of the parameters on machine performances. The clearest way to represent the considered analysis is by greyscale maps of the optimisation objectives versus only two parameters at a time, while the other parameters are set to their values defined analytical step.

Mean axial force. The mean axial force is strongly influenced by design parameters. As shown in Figure 13, a maximum force is reached for different α and β values from the initial analytical ones. In particular, the non-linear FE parameter analysis allows to take into account the maximum exploitation of the iron core, and the force maximisation is then obtained by increasing the permanent magnet length and the slot width. In Figure 14 the influence of γ and δ is reported. In this case the main role is played by the parameter γ. The FE analysis suggests a solution where cursor height is about twice that of the stator. In few words, the FE analysis shows that mean axial force improvements can be obtained by increasing active parts of the motor, with the maximum exploitation of the core material. It is important to point out that these results take into account thermal and demagnetisation constrains.

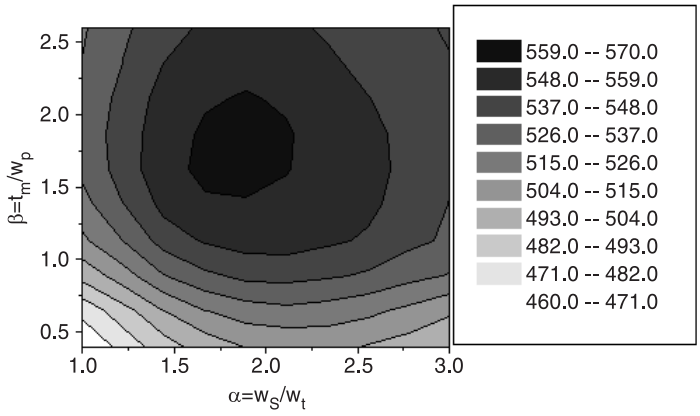

Figure 13.
Greyscale map of mean axial force versus α and β

Ripple force. The ripple force behaviour is easy to understand considering that minimum ripple force value occurs when motor anisotropy decreases. This effect is mainly due to the increment of stator tooth width (proportional to $1/\alpha$) and of cursor pole length (proportional to $1/\beta$) as shown in Figure 15, while the reduction of the cursor diameter (proportional to $1/\gamma$) corresponds to lower mean and ripple force as shown in Figure 16.

Global fuzzy. In the considered motor optimisation the main objective is represented by the mean axial force while the ripple force has been assumed as less important. These assumptions lead to the fuzzy sets reported in Figures 17 and 18. The values used in force membership function are obtained from analytical design while the ones for ripple force are obtained from some parametric analysis. In this case the maximum global fuzzy is mainly governed by the mean axial force fuzzy and the design configuration is near to that one which maximise this objective (as shown in Figures 19 and 20).

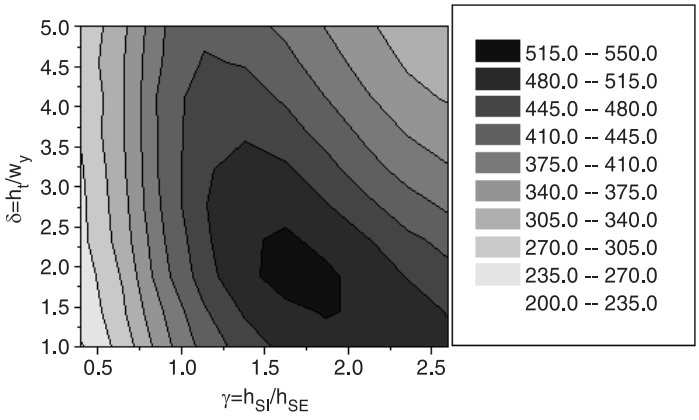

Figure 14.
Greyscale map of mean axial force versus γ and δ

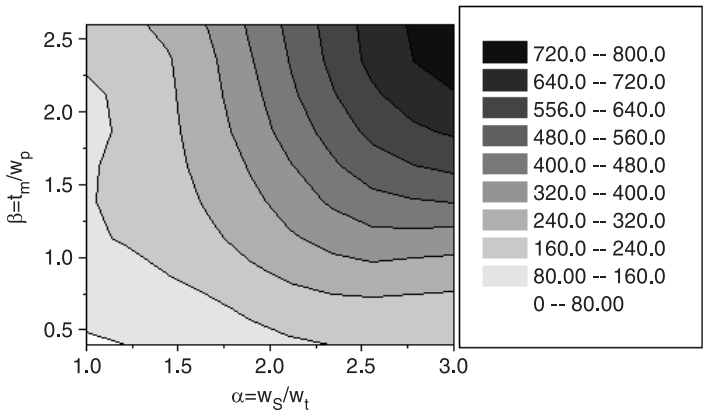

Figure 15.
Greyscale map of ripple axial force versus α and β

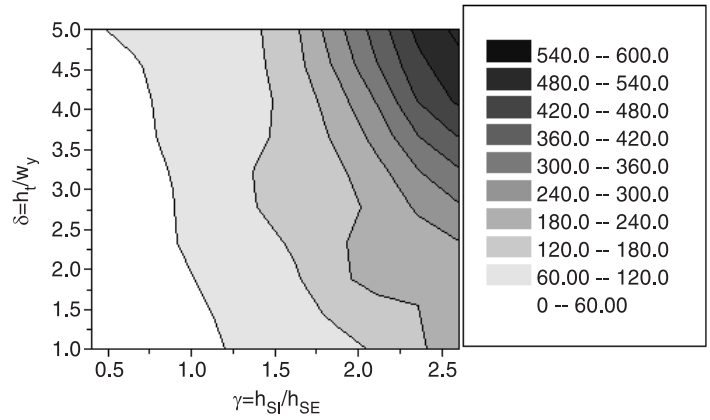

Figure 16.
Greyscale map of ripple axial force versus γ and δ

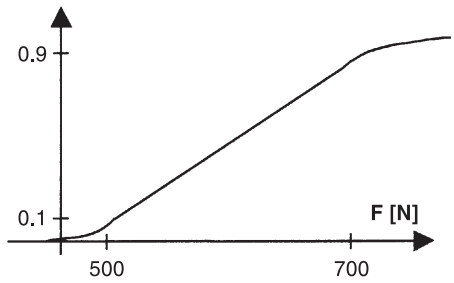

Figure 17.
Fuzzy set for the mean axial force

2. Optimisation results

Starting from the configuration suggested by the analytical method, the optimisation procedure leads to a new configuration, according to the results shown in the previous parameter analysis. Parameter behaviour and global fuzzy versus number of iterations are reported in Figures 21 and 22, while

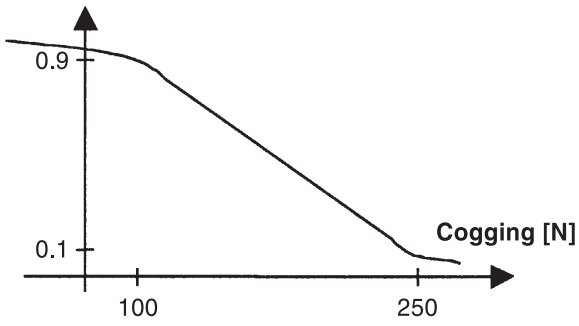

Figure 18.
Fuzzy set for the ripple ripple force

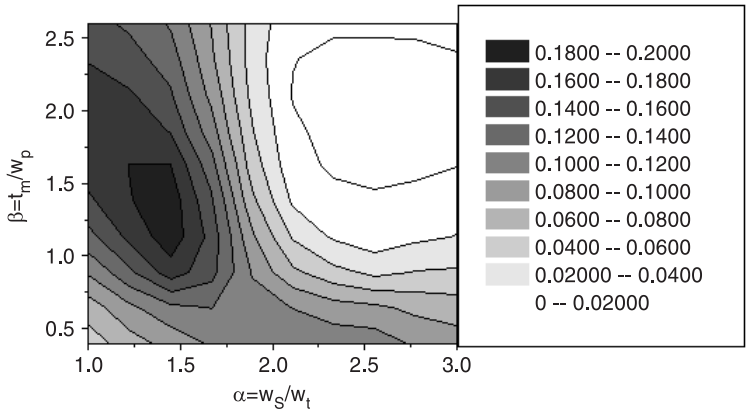

Figure 19.
Greyscale map of global fuzzy versus α and β

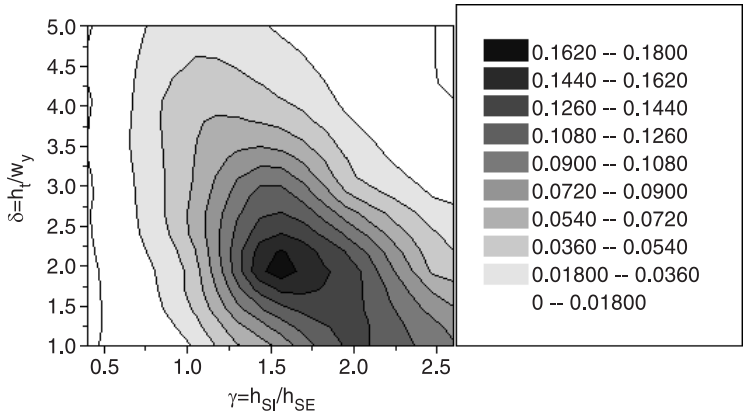

Figure 20.
Greyscale map of global fuzzy versus γ and δ

initial and final configuration parameters are compared in Tables II and III. Parameter behaviour confirms that the FE optimisation tends to increase the exploitation of the magnetic circuit, increasing the magnet axial length (β) and the slot area (α and β). Finally, Figure 24 shows the cross section of the motor in the initial and the final configurations.

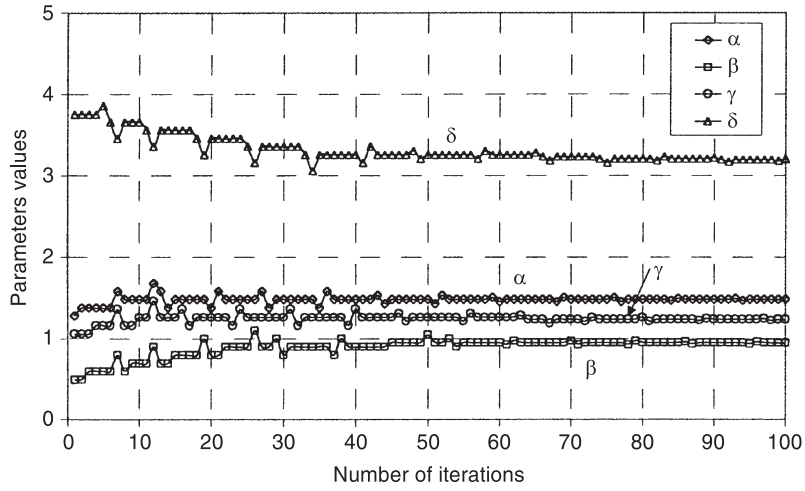

Figure 21.
Parameter behaviour versus number of iterations

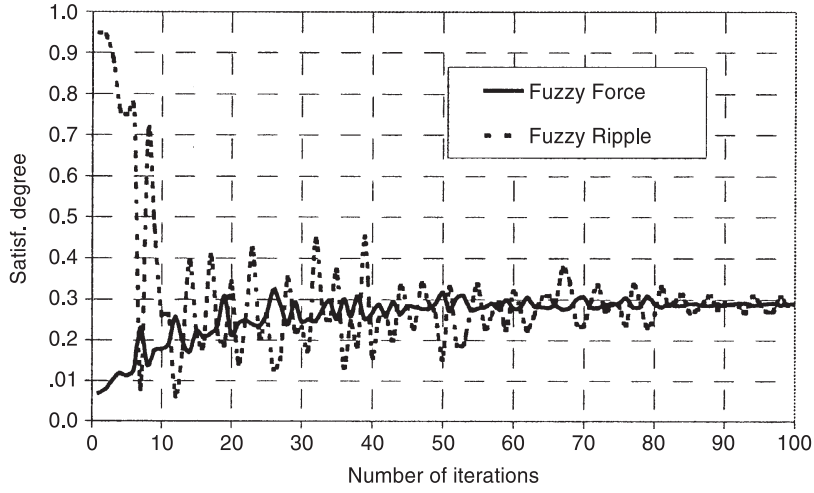

Figure 22.
Global fuzzy behaviour versus number of iterations

	Initial configuration	Final configuration
Alfa	1.28	1.48
Beta	0.50	0.95
Gamma	1.06	1.24
Delta	3.76	3.21

Table II.
Optimisation parameter: initial and final configuration

5. FEM optimisation design of slotless TLPM motor

The behaviour of a slotless TLPM motor is characterised by a practical null ripple force. In this case the problem becomes scalar and the optimisation process does not require a scalarisation procedure.

As proposed for the slotted motor optimisation, suitable ratios between motor dimensions, reported in Figure 23, have been introduced together with external volume constraint. All the motor dimensions are then calculated from the introduced optimisation parameter through the formula reported in Appendix B.

1. Parameter analysis

Mean axial force. The mean axial force is strongly influenced by design parameters. Figures 25 and 26 show that δ and γ given by the analytical method (γ = 2 and δ = 2.125) lead the axial force close to its maximum; these values

	Initial configuration		Final configuration	
	Actual value	Satisf. degree	Actual value	Satisf. degree
Force	482	0.0692	559	0.288
Ripple	74.9	0.949	205	0.291

Table III.
Optimisation objectives

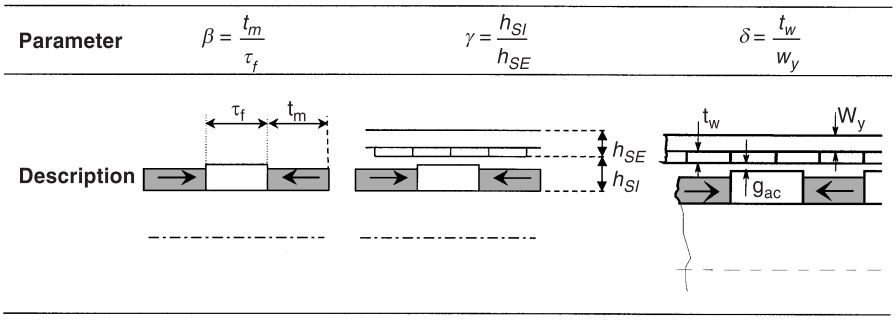

Figure 23.
Optimisation parameter

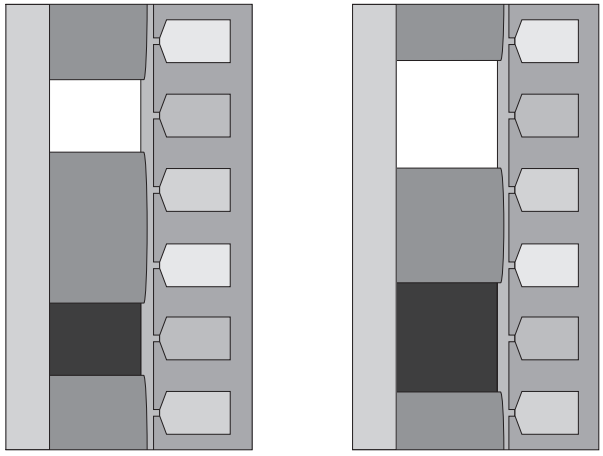

Figure 24.
Section of the motor

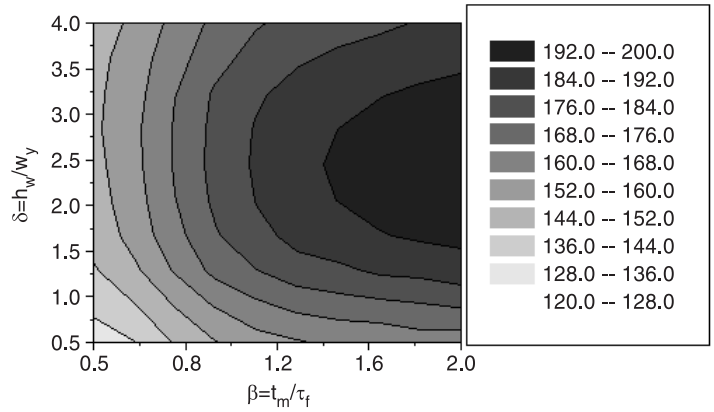

Figure 25.
Greyscale map of mean axial force versus β and δ

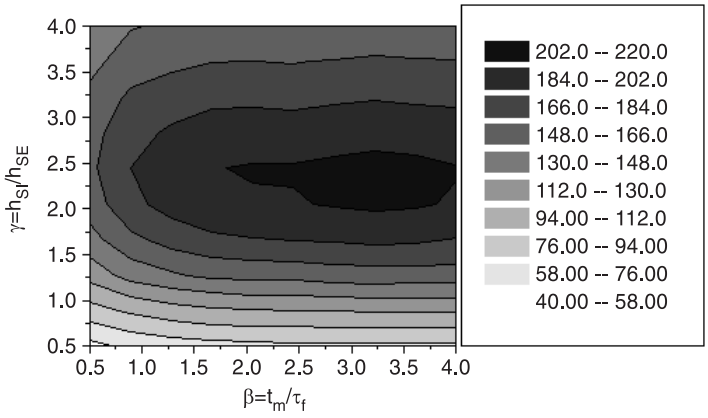

Figure 26.
Greyscale map of mean axial force versus β and γ

correspond to a stator winding thickness of about twice the yoke height and to a radial dimension of the active part of the cursor of about twice the stator radial dimension. Increasing the β coefficient, an increment of motor axial force occurs but, after a certain value of β, the improvement become negligible. Also in this case, as observed for the slotted structure, the maximum force is obtained for an axial magnet length two or three times the pole length.

2. Optimisation results

Behaviour of parameters and global fuzzy throughout the optimisation process are reported in Figures 27 and 28, while initial and final configuration parameters are compared in Tables IV and V. As observed for the slotted structure, the parameter behaviour confirms that the FE optimisation tends to increase the exploitation of the magnetic circuit, increasing the magnet axial length (β) and the radius of cursor (γ). Finally, Figure 29 shows the cross section of the motor in the two configurations.

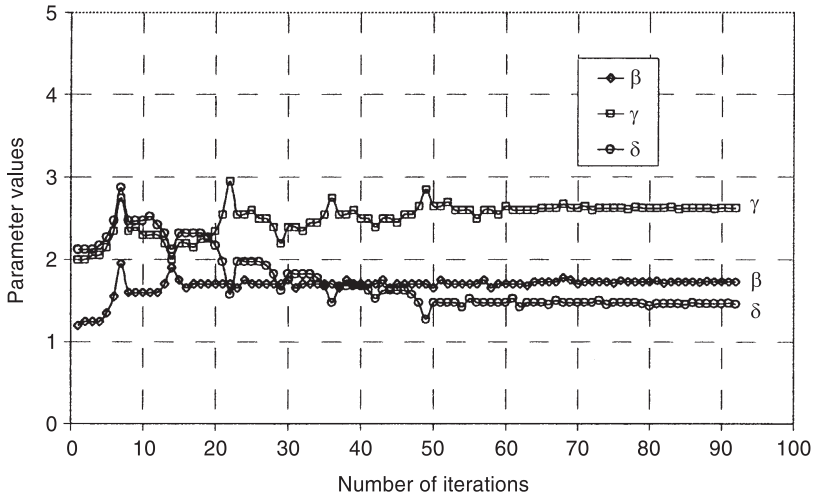

Figure 27.
Parameter behaviour versus number of iterations

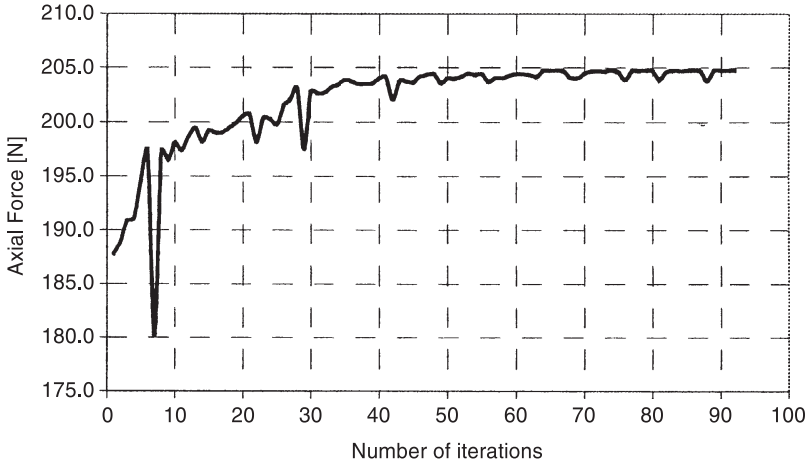

Figure 28.
Axial force behaviour versus number of iterations

	Initial configuration	Final configuration
Beta	1.20	1.73
Gamma	2.00	2.63
Delta	2.13	1.46

Table IV.
Optimisation parameter: initial and final configuration

	Initial configuration	Final configuration
Force	188	205

Table V.
Optimisation objective

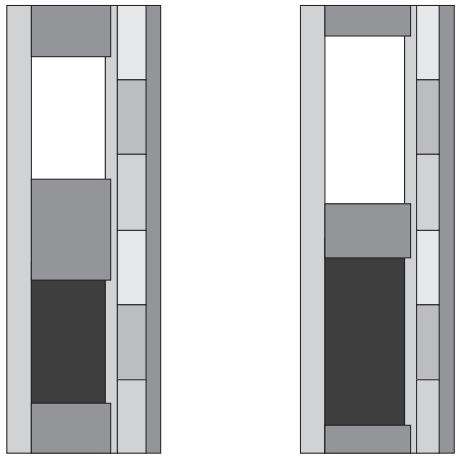

Figure 29.
Section of the motor

6. Conclusions

In this paper the optimisation of a tubular linear motor, with interior permanent magnets and two different stator structures (slotted and slotless), has been presented. The proposed procedure is composed of a first analytical procedure, which defines a first set of geometric parameters which are introduced in an automated design optimisation based on FEM performances evaluation. The final configurations, obtained for the two kinds of stator structures, present improvement of the axial force given by the analytical method (about 15 percent for the slotted stator and about 10 percent for the slotless one). These improvements are reached through an increment of permanent magnet, which produces an highest exploitation of the iron core in terms of magnetic field density. Moreover, several runs from different initial points have shown that more than one optimal configuration design is reached at the end of the optimisation procedure, able to satisfy the performance requirements. Finally, it is important to point out that other performances and phenomena have not been taken into account as end effect (Zhu *et al.*, 1997) or eddy currents (Sangha and Rodger, 1994), which can play an important role in the design of short machines with massive magnetic core and will be modelled in the future research activity on this subject.

References

Bianchi, N., Bolognani, S. and Tonel, F. (2000), "Design considerations for a tubolar linear PM motor for servo drives", *9th International Power Electronics and Motion Control Conference, EPE-PEMC 2000*, Kosice, Slovak Republic, 5-7 September.

Canova, A., Chiampi, M., Ragusa, C. and Repetto, M. (1998), "Automated design of magnetic circuit of induction machines using multiobjective optimisation techniques and finite element method", *IOS Press. Int. Journal of Applied Electromagnetics and Mechanics*, No. 9, pp. 1-9.

Chiampi, M., Ragusa, C. and Repetto, M. (1996), "Fuzzy approach for multiobjective optimisation in magnetics", *IEEE Trans. MAG.*, Vol. 32, pp. 1234-7.

Sangha, P.S. and Rodger, D. (1994), "Design and analysis of voltage fed axis symmetric actuators", *IEEE Trans. MAG.*, Vol. 30 No. 5, pp. 3240-3.

Zhu, Z.Q., Xia, Z.P., Howe, D. and Mellor, P.H. (1997), "Reduction of cogging force in slotless linear permanent magnet motors", *IEE Proc., Electr. Power Appl.*, Vol. 144, pp. 277-82.

Appendix A

Stator slot parameter: slot and tooth width

The ratio between stator slot dimensions is chosen as parameter:

$$\alpha = \frac{w_s}{w_t}$$

the bond is:

$$w_s + w_t = {}^{\tau}/_{3}$$

then combining the two equations:

$$\begin{cases} w_s = \left(\dfrac{\alpha}{1+\alpha}\right)\dfrac{\tau}{3} \\ w_t = \left(\dfrac{1}{1+\alpha}\right)\dfrac{\tau}{3} \end{cases}$$

where the theoretical limits of α are:

$$0 \leq \alpha \leq \infty$$

Stator slot parameter: slot and yoke height

The ratio between stator slot height and the yoke thickness is chosen as parameter:

$$\delta = \frac{h_t}{w_y}$$

the bond is:

$$h_t + w_y = h_s$$

where h_s is the stator height and is equal to: $h_s = \frac{(D_e - D)}{2}$

then combining the two equations:

$$\begin{cases} h_t = \left(\dfrac{\delta}{1+\delta}\right)h_s \\ w_y = \left(\dfrac{1}{1+\delta}\right)h_s \end{cases}$$

where the theoretical limits of δ are:

$$0 \leq \delta \leq \infty$$

Cursor pole parameter

The ratio between the magnet length t_m and the pole length $\tau_f = \tau - t_m$ is chosen as parameter:

$$\beta = \frac{t_m}{\tau_f}$$

the bond is:

$$t_m + \tau_f = \tau$$

then combining the two equations:

$$\begin{cases} t_m = \left(\dfrac{\beta}{1+\beta}\right)\tau \\ \tau_f = \left(\dfrac{1}{1+\beta}\right)\tau \end{cases}$$

where the theoretical limits of β are:

$$0 \leq \beta \leq \infty$$

Stator-cursor parameter

Keeping constant the inner and the external diameters, the designer has to choose how to share the total volume between stator and cursor. The ratio between the cursor radial dimension:

$$h_{SI} = D - D_0$$

and the stator radial dimension:

$$h_{SE} = D_e - D$$

is defined as parameters:

$$\gamma = \frac{h_{SI}}{h_{SE}}$$

It is important to observe that airgap thickness dimensions: h_δ and h_{int} are keep constant in the optimisation procedure ($h_\delta = 1\text{mm}$ and $h_{int} = 1\text{mm}$).

The bonds are:

$$h_{SI} + h_{SE} = \frac{(D_e - D_0)}{2}$$

$$h_{SI} \geq D - D_m \text{ or } h_{SI} \geq h_{int} + h_\delta$$

Combining the equations:

$$\begin{cases} h_{SI} = \left(\dfrac{\gamma}{1+\gamma}\right)(D_e - D_0) \\ h_{SI} = \left(\dfrac{1}{1+\gamma}\right)(D_e - D_0) \end{cases}$$

Finally, the theoretical limits of γ are:

$$\frac{h_{int} + h_\delta}{[(D_e - D_0) - (h_{int} + h_\delta)]} \leq \gamma \leq \infty$$

Appendix B

Stator parameter: winding and yoke height

The ratio between stator slot height and the yoke thickness is chosen as parameter:

$$\delta = \frac{t_w}{w_y}$$

the bond is:

$$t_w + w_y = h_s$$

where h_S is the stator height and is equal to: $h_S = \frac{(D_e - D)}{2}$

then combining the two equations:

$$\begin{cases} t_w = \left(\dfrac{\delta}{1+\delta}\right) h_S \\ w_y = \left(\dfrac{1}{1+\delta}\right) h_S \end{cases}$$

where the theoretical limits of are:

$$0 \leq \delta \leq \infty$$

Cursor pole parameter

The ratio between the magnet t_m length and the pole length $\tau_f = \tau - t_m$ is defined in the same way as the slotted motor:

$$\beta = \frac{t_m}{\tau_f}$$

Stator-cursor parameter

Keeping constant the inner and the external diameters, the ratio between the cursor radial dimension:

$$h_{SI} = D - D_0$$

and the stator radial dimension:

$$h_{SE} = D_e - D$$

is defined the same way as the slotted motor:

$$\gamma = \frac{h_{SI}}{h_{SE}}$$